Proceedings of the 7th GACM Colloquium on Computational Mechanics
for Young Scientists from Academia and Industry
October 11-13, 2017 in Stuttgart, Germany

A method for the elimination of shear locking effects in an isogeometric Reissner-Mindlin shell formulation

Georgia Kikis[1]*, Wolfgang Dornisch[2] and Sven Klinkel[1]

Micro Abstract
Shell elements for slender structures based on a Reissner-Mindlin approach struggle in pure bending problems. The stiffness of such structures is overestimated due to the transversal shear locking effect. Here, an isogeometric Reissner-Mindlin shell element is presented, which uses adjusted control meshes for the displacements and rotations in order to create a conforming interpolation of the pure bending compatibility requirement. The method is tested for standard numerical examples.

[1]Chair of Structural Analysis and Dynamics, RWTH Aachen University, Aachen, Germany
[2]Chair of Applied Mechanics, University of Kaiserslautern, Kaiserslautern, Germany
***Corresponding author**: kikis@lbb.rwth-aachen.de

Introduction

Isogeometric analysis (IGA) has many benefits due to the, in CAD commonly used, NURBS shape functions. The high continuity of these functions reduces the computational effort for complex structures and unifies the design and analysis process. However, IGA formulations suffer from locking which adds artificial stiffness and leads to an underestimation of the deformations. The use of higher order shape functions and reduced integration only alleviates the problem. Other methods have been adopted from FEM, such as the Discrete Strain Gap method (DSG), the enhanced assumed strain method (EAS) and the B-bar method. Here, the focus is on a method proposed by Beirão da Veiga [1] for the elimination of transverse shear locking in Reissner-Mindlin plates. The approach is extended to the Reissner-Mindlin shell from Dornisch [2].

1 Isogeometric Reissner-Mindlin shell analysis

1.1 Reissner-Mindlin shell formulation

The Reissner-Mindlin shell which was proposed by Dornisch [2] is derived from continuum mechanics and described only by its midsurface. The thickness direction is defined by the director vector. The reference director vector $\boldsymbol{D}$ coincides with the normal vector of the shell surface and has the length $|\boldsymbol{D}(\xi^\alpha)| = 1$. Since the shell element is linear, a difference vector formulation can be applied for the definition of the deformed director vector $\boldsymbol{d} = \boldsymbol{D} + \boldsymbol{b}$. The difference vector $\boldsymbol{b} = \boldsymbol{\omega} \times \boldsymbol{D}$ is constructed by the vector cross product between the rotational parameter of the shell midsurface $\boldsymbol{\omega}$ and the reference director vector. Its derivative with respect to the parametric coordinates ξ_α is given as follows

$$\boldsymbol{b}_{,\alpha} = \boldsymbol{\omega}_{,\alpha} \times \boldsymbol{D} + \boldsymbol{\omega} \times \boldsymbol{D}_{,\alpha} \tag{1}$$

The shell strains that result from the linearized Green-Lagrange strain tensor are sumed up in the vector $\boldsymbol{\varepsilon} = \begin{bmatrix}\varepsilon_{11} & \varepsilon_{22} & 2\varepsilon_{12} & \kappa_{11} & \kappa_{22} & 2\kappa_{12} & \gamma_1 & \gamma_2\end{bmatrix}^T$ where $\varepsilon_{\alpha\beta}$ are the membrane strains,

$\kappa_{\alpha\beta}$ the curvature of the shell and γ_α the shear strains:

$$\varepsilon_{\alpha\beta} = \frac{1}{2}(\boldsymbol{X}_{,\alpha} \cdot \boldsymbol{u}_{,\beta} + \boldsymbol{X}_{,\beta} \cdot \boldsymbol{u}_{,\alpha}) \tag{2}$$

$$\kappa_{\alpha\beta} = \frac{1}{2}(\boldsymbol{X}_{,\alpha} \cdot \boldsymbol{b}_{,\beta} + \boldsymbol{X}_{,\beta} \cdot \boldsymbol{b}_{,\alpha} + \boldsymbol{D}_{,\alpha} \cdot \boldsymbol{u}_{,\beta} + \boldsymbol{D}_{,\beta} \cdot \boldsymbol{u}_{,\alpha}) \tag{3}$$

$$\gamma_\alpha = \boldsymbol{X}_{,\alpha} \cdot \boldsymbol{b} + \boldsymbol{u}_{,\alpha} \cdot \boldsymbol{D} \tag{4}$$

The weak form of equilibrium which is used for the shell formulation is given as:

$$G(\boldsymbol{v}, \delta\boldsymbol{v}) = \int_\Omega \delta\boldsymbol{\varepsilon}^T \cdot \boldsymbol{\sigma} \; dA - \int_\Omega \delta\boldsymbol{v}^T \bar{\boldsymbol{p}} \; dA - \int_{\Gamma_t} \delta\boldsymbol{v}^T \bar{\boldsymbol{t}} \; ds = \boldsymbol{0} \tag{5}$$

with $\bar{\boldsymbol{p}}$ the surface loads, $\bar{\boldsymbol{t}}$ the boundary tractions and $\boldsymbol{v} = \begin{bmatrix} u_1 & u_2 & u_3 & \beta_1 & \beta_2 \end{bmatrix}^T$ the solution variable. The stress resultants $\boldsymbol{\sigma}$ are later replaced in the weak form using Hookes Law $\boldsymbol{\sigma} = \mathbb{C} \cdot \boldsymbol{\varepsilon}$.

1.2 NURBS-based isogeometric analysis

The shell surface is described using Non-Uniform Rational B-Splines N_I. The position vector $\boldsymbol{X}$ of an arbitrary physical point on the NURBS surface and its derivative is interpolated as follows

$$\boldsymbol{X}(\xi_1, \xi_2) = \sum_{I=1}^{n_{en}} N_I(\xi_1, \xi_2)\boldsymbol{X}_I \qquad \frac{\partial}{\partial \xi_\alpha}\boldsymbol{X}(\xi_1, \xi_2) = \sum_{I=1}^{n_{en}} \frac{\partial N_I(\xi_1, \xi_2)}{\partial \xi_\alpha}\boldsymbol{X}_I \tag{6}$$

Analogously, the interpolation of the nodal director vectors $\boldsymbol{D}$ and its derivative $\boldsymbol{D}_{,\alpha}$ is

$$\boldsymbol{D}(\xi_1, \xi_2) = \sum_{I=1}^{n_{en}} N_I(\xi_1, \xi_2)\boldsymbol{D}_I \qquad \boldsymbol{D}_{,\alpha}(\xi_1, \xi_2) = \sum_{I=1}^{n_{en}} N_{I,\alpha}(\xi_1, \xi_2)\boldsymbol{D}_I \tag{7}$$

The difference vector $\boldsymbol{b}$ and its derivative are described using the rotational parameter $\boldsymbol{\omega}$, see (1). Furthermore, there exist a connection between $\boldsymbol{\omega}$ and the nodal rotations $\boldsymbol{\beta}_I$

$$\boldsymbol{\omega}(\xi_1, \xi_2) = \sum_{I=1}^{n_{en}} \boldsymbol{T}_{3I} N_I(\xi_1, \xi_2)\boldsymbol{\beta}_I \qquad \boldsymbol{\omega}_{,\alpha}(\xi_1, \xi_2) = \sum_{I=1}^{n_{en}} \boldsymbol{T}_{3I} N_{I,\alpha}(\xi_1, \xi_2)\boldsymbol{\beta}_I \tag{8}$$

For a smooth surface the transformation matrix $\boldsymbol{T}_{3I}$ includes only two nodal basis sytem vectors of the reference configuration $\boldsymbol{T}_{3I} = \begin{bmatrix} \boldsymbol{A}_{1I} & \boldsymbol{A}_{2I} \end{bmatrix}$. The third one $\boldsymbol{A}_{3I}$ is not included in order to avoid zero energy modes from drilling rotations. The basis is computed using the method of optimal nodal basis system from Dornisch [2].

1.3 Adjusted approximation spaces against transverse shear locking

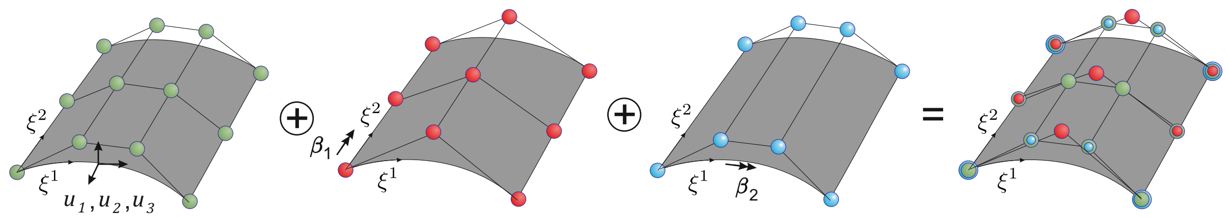

Figure 1. Adjusted approximation spaces for u_i and β_α and the resulting global mesh.

The root of the transverse shear locking in pure bending problems lies in the compatibility requirements, which are for instance for plane surfaces as follows

$$u_{3,1} + \beta_1 = 0 \qquad u_{3,2} + \beta_2 = 0 \tag{9}$$

and must be fullfilled, especially for Kirchhoff-Love like shells. The use of the same shape functions for the displacements u_i and the rotations β_α leads to a mismatch in (9) which creates the locking effect. Thus, transverse shear locking is a numerical error not a physical error. Beirão da Veiga et al. [1] proposed a simple but effective method for treating this discrepancy, which uses different shape functions for u_i and β_α with compatible polynomial degrees. This neccesitates seperate control meshes for the displacements and the rotations, see Figure 1. The meshes of the rotations β_1 and β_2 have a ploynomial degree less than u_i in the relevant direction. It is important to mention that the starting geometry is the same for all three meshes. Only by applying different levels of refinement, the new control meshes are created. Thus, the isogeometric concept still holds. The solution of the weak formulation requires the implementation of a global mesh, which includes the control points from all three meshes. In this manner, the new mesh has control points with three, four or five degrees of freedom. The shell strains of the new global mesh can be devided in three parts, each of which arises from one of the three control meshes:

$$\delta\boldsymbol{\varepsilon}_I = \boldsymbol{B}_I^{u^T} \cdot \delta\boldsymbol{u}_I + \boldsymbol{B}_I^{\beta_1^T} \cdot \delta\beta_{1I} + \boldsymbol{B}_I^{\beta_2^T} \cdot \delta\beta_{2I} \tag{10}$$

$\boldsymbol{B}_I^u$ is a 3x8 Matrix which includes the shape functions N_I^u from (6) and (7) whereas $\boldsymbol{B}_I^{\beta_1^T}$ and $\boldsymbol{B}_I^{\beta_2^T}$ have the dimension 1x8 and contain the shape functions $N_I^{\beta_1}$, $N_I^{\beta_2}$ and the discrete nodal basis systems $A_{1I}^{\beta_1}$, $A_{2I}^{\beta_2}$ from (8). The new weak form based on the global control mesh reads

$$G(\boldsymbol{v}, \delta\boldsymbol{v}) = \sum_{e=1}^{numel} \left(\sum_{I}^{n_{ges}} \sum_{J}^{m_{ges}} \delta\boldsymbol{v}_I^T \int \begin{bmatrix} \boldsymbol{B}_I^{u^T} \cdot \mathbb{C} \cdot \boldsymbol{B}_J^u & \boldsymbol{B}_I^{u^T} \cdot \mathbb{C} \cdot \boldsymbol{B}_J^{\beta_1} & \boldsymbol{B}_I^{u^T} \cdot \mathbb{C} \cdot \boldsymbol{B}_J^{\beta_2} \\ \boldsymbol{B}_I^{\beta_1^T} \cdot \mathbb{C} \cdot \boldsymbol{B}_J^u & \boldsymbol{B}_I^{\beta_1^T} \cdot \mathbb{C} \cdot \boldsymbol{B}_J^{\beta_1} & \boldsymbol{B}_I^{\beta_1^T} \cdot \mathbb{C} \cdot \boldsymbol{B}_J^{\beta_2} \\ \boldsymbol{B}_I^{\beta_2^T} \cdot \mathbb{C} \cdot \boldsymbol{B}_J^u & \boldsymbol{B}_I{}^{\beta_2^T} \cdot \mathbb{C} \cdot \boldsymbol{B}_J^{\beta_1} & \boldsymbol{B}_I^{\beta_2^T} \cdot \mathbb{C} \cdot \boldsymbol{B}_J^{\beta_2} \end{bmatrix} dA \cdot \boldsymbol{v}_J \right.$$

$$\left. - \delta\boldsymbol{v}_e^T \cdot \left(\int \begin{bmatrix} N_I^u & 0 & 0 & 0 & 0 \\ 0 & N_I^u & 0 & 0 & 0 \\ 0 & 0 & N_I^u & 0 & 0 \\ 0 & 0 & 0 & 0 & 0 \\ 0 & 0 & 0 & 0 & 0 \end{bmatrix} \cdot \begin{bmatrix} q_x \\ q_y \\ q_z \\ 0 \\ 0 \end{bmatrix} dA - \boldsymbol{f}_{boun}^{ext} \right) \right) = \boldsymbol{0} \tag{11}$$

2 Numerical examples

2.1 Skew plate

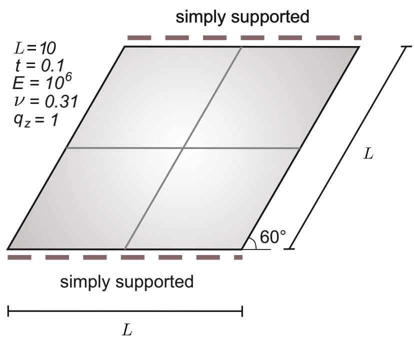

Figure 2. Razzaque's skew plate subjected to a uniformly distributed load.

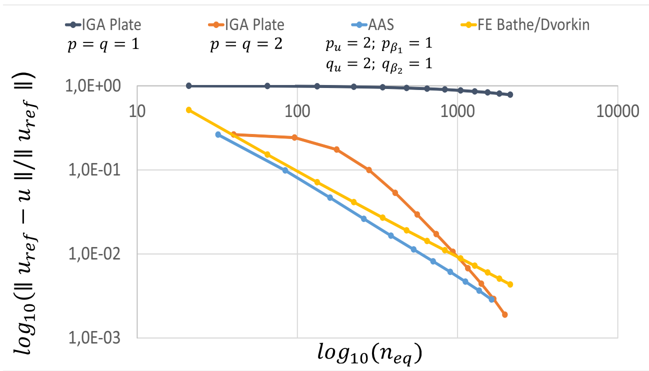

Figure 3. Error for center deflection with n_{eq} the number of equations for the solution.

The skew plate, see Fig. 2, examines the sensitivity of an element to mesh disortions. For high slenderness it exhibits transverse shear locking. Fig. 3 shows the relative error of the deflection at the center of the plate. The proposed element with adjusted approximation spaces (AAS) is compared to an isogeometric Reissner-Mindlin plate (IGA Plate) and the Bathe/Dvorkin 4-node thin plate bending element (FE Bathe/Dvorkin) which already includes an anti locking mechanism. The standard IGA plate element clearly exhibits transverse shear locking for a low number of elements. The higher the number of elements get, the more the effect is alleviated. On the other hand, the AAS element is not affected by locking even for a low number of elements and shows a constant convergence rate. This rate is the same as for the FE Bathe/Dvorkin element. However, AAS compared to FE Bathe /Dvorkin has slightly better results due to the use of a higher polynomial degree for the displacements.

2.2 Partly clamped hyperbolic paraboloid

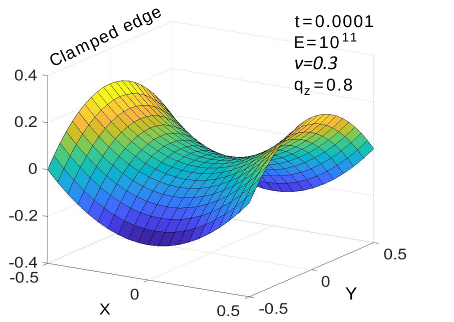

Figure 4. Partly clamped hyperbolic paraboloid.

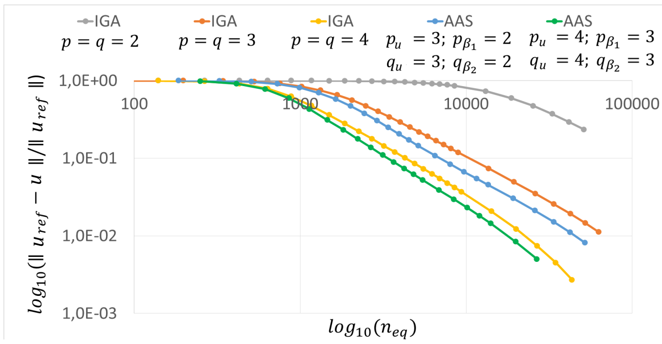

Figure 5. Error for deflection at $X = \frac{L}{2}$, $Y = 0$ with n_{eq} the number of equations for the solution.

The partly clamped hyperbolic paraboloid is bending dominated and a good example for the investigation of locking effects in shells. The problem consists of an partly clamped surface defined as $Z = X^2 - Y^2; (X, Y) \in [(-L/2; L/2)]^2$ which is loaded by self-weight, see Figure 4 The reference solution was adopted from [3] for a 48x24 mesh of MITC16 elements. In Figure 5 the L_∞ error norm of the deflection at point $X = \frac{L}{2}$, $Y = 0$ is given. The AAS element with p_u always shows a higher accuracy than its equivalent IGA element with $p = p_u$. Interesting is that the resulting convergence rates are almost the same for AAS and IGA, resulting in almost parallel error lines. The higher the polynomial degree the smaller the difference between the two lines, due to the alleviation of locking effects with higher order shape functions. It is important to mention that for curved shells, transverse shear locking usually occures simultaneously with other locking effects, such as membrane locking. These effects are not treated with this method.

Conclusions

In this work a method for the treatment of transverse shear locking effects in shell elements was proposed. The method uses adjusted approximation spaces for the displacements and rotations in order to fullfil the two compatibility requirements for pure bending. The method showed higher accuracy compared to the standard IGA element, even for skew geometries. Furthermore, it can compete with the element formulation of Bathe and Dvorkin.

References

[1] L. Beirão da Veiga, A. Buffa, C. Lovadina, M. Martinelli and G. Sangalli, An isogeometric method for the Reissner-Mindlin plate bending problem. *Comput. Meth. Appl. Mech. Engrg.*, Vol. 209-212: p.45-53, 2012.

[2] W. Dornisch, R. Müller and S. Klinkel, An efficient and robust rotational formulation for isogeometric Reissner-Mindlin shell elements. *Comput. Meth. Appl. Mech. Engrg.*, Vol. 303: p.1-34, 2016.

[3] K.J. Bathe, A. Iosilevich and D. Chapelle, An evaluation of the MITC shell elements. *Computers and Structures*, Vol. 75: p.1-30, 2000.